Technical Report No. 21

SACLANT ASW
RESEARCH CENTER

A THEORETICAL AND EXPERIMENTAL STUDY OF THE KINEMATICS OF A CORING TUBE ACCELERATED IN WATER BY HYDROSTATIC PRESSURE

by

A. KERMABON

1 March 1964

NATO

VIALE SAN BARTOLOMEO, 92
LA SPEZIA, ITALY

This document is released to a NATO Government at the direction of the SACLANTCEN subject to the following conditions:

1. The recipient NATO Government agrees to use its best endeavours to ensure that the information herein disclosed, whether or not it bears a security classification, is not dealt with in any manner (a) contrary to the intent of the provisions of the Charter of the Centre, or (b) prejudicial to the rights of the owner thereof to obtain patent, copyright, or other like statutory protection therefor.

2. If the technical information was originally released to the Centre by a NATO Government subject to restrictions clearly marked on this document the recipient NATO Government agrees to use its best endeavours to abide by the terms of the restrictions so imposed by the releasing Government.

TECHNICAL REPORT NO. 21

SACLANT ASW RESEARCH CENTRE
Viale San Bartolomeo 92
La Spezia, Italy

A THEORETICAL AND EXPERIMENTAL STUDY OF THE KINEMATICS OF A CORING TUBE ACCELERATED IN WATER BY HYDROSTATIC PRESSURE

By

A. Kermabon

1 March 1964

APPROVED FOR DISTRIBUTION

HENRIK NØDTVEDT
Director

A THEORETICAL AND EXPERIMENTAL STUDY OF THE KINEMATICS OF A CORING TUBE ACCELERATED IN WATER BY HYDROSTATIC PRESSURE

By

A. Kermabon

Summary

The implosion at great marine depths of a system composed of a light tube, which is closed at one end by a light cap and at the other by a heavy piston, is examined theoretically and experimentally. Special attention has been given to the downward acceleration of the tube.

This accelerated tube can be used to core deep sea sediments, and a study of the penetration of the tube in normal sediments has been made. With this new coring device, it should be possible to obtain long cores with relatively light equipment.

A small scale model has been tested; it has given encouraging results. Sea tests of a full scale prototype have just started.

Some technological details are given, but the present design will be subject to many improvements and changes.

1. INTRODUCTION

Cores of deep sea sediments are normally obtained by a tube, which is attached to a large heavy mass and allowed to fall freely a few metres above the sediment to be cored. The equipment is rough and needs little maintenance; however, manoeuvring heavy weights at sea is always a delicate and dangerous operation and, unless the masses are very large, the energy involved is limited. The energy may be increased by increasing the drop distance, but the drag coefficient of the driving mass (always large in diameter) limits the speed.

Some oceanographers have tried to use the hydrostatic pressure at the bottom of the sea to force a corer into a hard bottom. In 1927, M. Knudsen (Ref. 1) reported on a sampler for a hard bottom, and in 1940 Pettersson and Kullenberg (Ref. 2) published a paper in Nature on a vacuum core sampler. However, neither was able to avoid the "sucking effect" of the sediments during penetration and the projects were abandoned. In 1941, Piggot (Ref. 3) designed a corer that was driven into the sediments by the forces created by an explosion of black powder. The coring tube, driven at high speed into the sediments, obtained cores up to 3 metres in length. The equipment was relatively light; however, aside from the fact that handling of explosives at sea is dangerous, most of the released energy was used to counterbalance the external pressure.

This report proposes a system that uses hydrostatic pressure to accelerate a coring tube, suspended just above the sediments, and to gain, in this way, in kinetic energy what a light equipment loses in potential energy. The proposed system is mechanically simple, and the coring tube is utilized as a reservoir of energy (air at atmospheric pressure) during the propulsive period. The corer is released well above the sediments and, in this way, any "suction effect" of the sediments is avoided.

2. PRINCIPLE OF TUBE ACCELERATOR

Figure 1 shows the mechanics of the system. The tube contains a vacuum or air at atmospheric pressure and is made watertight by a cap at one end and a piston at the other. The cap may move upward freely, but its downward movement is prevented by a shoulder; the piston is held fixed in the tube by a shearing pin.* The piston has a large mass as compared to the total mass $m_0 + m_1$ of the cap and tube.

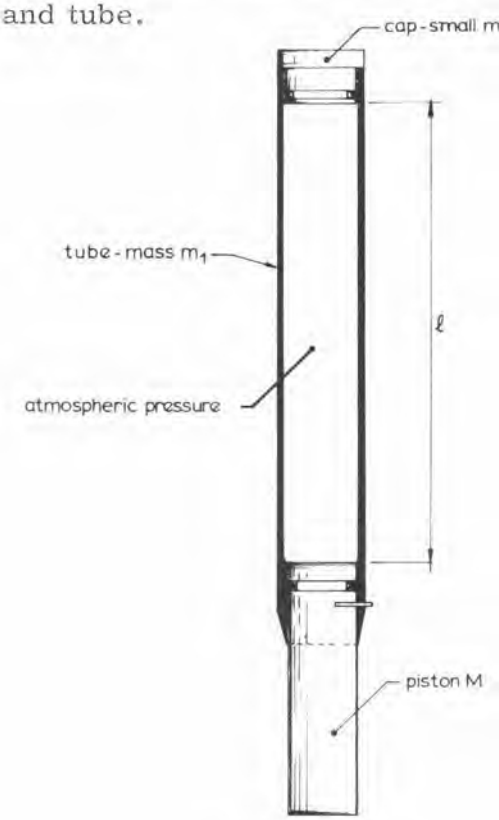

Fig. 1 The Tube Accelerator - Assembly Principle

Now let us study the system when it is submitted to the external pressure existing at great marine depths. The external hydrostatic pressure forces on the tube-cap-piston group are statically counterbalanced by the internal forces of the rigid mechanical system. When the shearing pin is broken and the piston is free to move in the tube, the mechanical group, still under the influence of the same external forces, will no longer possess internal counterbalancing forces in the vertical plane. (With the exception of the small force produced by the compression of the air, which was stored at atmospheric pressure in the tube.) Two movements will then occur:

1. The tube will move downward due to the force applied to the cap
2. The piston will be forced upward in the tube by the external pressure.

---

*In actual operation, the piston is locked to the tube by a mechanical quick-releasing device.

Since the piston is long, the friction force of the piston in the water will not differ greatly from that of the tube. Since the entire system is submitted to external forces only (if the effects of friction are disregarded), one can state the conservation of kinetic moments at any instant as

$$MV = (m_1 + m_0)\, v$$

where

M	=	the mass of the piston
V	=	instantaneous speed of the piston
m_1	=	mass of the tube
m_0	=	mass of the cap
v	=	instantaneous speed of the tube

Let m represent $m_1 + m_0$, and the tube speed may be shown constant at about M/m times the speed of the piston (disregarding friction). Similarly, the tube will move in vertical distance M/m times the distance moved by the tube (again disregarding friction) during the propulsion phase.

When the air inside the tube has been compressed by the piston, the differential energy, due to the pressure difference between interior and exterior, ceases to exist. Since the internal and external vertical forces are equal, the kinetic energy of the piston is sufficient to carry away the lightweight cap at the top of the tube. When this occurs, only the tube continues toward the bottom at a high speed, while the piston moves upward at a slower speed. The kinetic energy acquired by the tube is sufficient to cause it to penetrate the sediments at a very high speed; thus, it is possible to obtain long cores with relatively light equipment.

3. DYNAMICS OF THE PROPULSION PHASE

The movement of the tube and cap, after the release of the piston, is considered. Let

m = mass (cap + tube)

d = mass density of cap and tube

x = distance traveled by the tube from the moment the piston is released until the moment t

p_o = external pressure

S = inside section of the tube

k = drag coefficient of the tube. Dimension ML^{-1}

ρ = specific mass of water

Then the equation of motion can be written

$$m\frac{d^2x}{dt^2} = mg\left(1 - \frac{1}{d}\right) - k\left(\frac{dx}{dt}\right)^2 + p_o S - \frac{\rho}{2} S \left(\frac{dx}{dt}\right)^2 - x\,\rho g\, S \qquad (1)$$

The term $p_o S$ has a value of approximately 10,000 kg at 2500 m depth and, by comparison, the term $mg\left(1 - \frac{1}{d}\right) \approx 30$ kg can be neglected.

$-k\left(\frac{dx}{dt}\right)^2$ is the resistance of a moving body in water due to drag and water friction

$p_o S$ is the initial force applied to the cap at time zero

$-\frac{\rho}{2} S \left(\frac{dx}{dt}\right)^2$ is the restrictive term taking into account that, during the movement, the initial pressure p_o, which is applied to the cap, is not constant, since some potential energy is transformed into kinetic energy.

$-x\rho gS$ is the variation of potential energy. Since this term is small (because x is small), it will be ignored.

The term

$$S\left[p_o - \frac{\rho}{2}\left(\frac{dx}{dt}\right)^2 - x\rho g\right]$$

is derived from Bernouilli's theorem. The amount of water in direct contact with the cap follows, more or less, this laminar law of flow.

If we consider that p_o static pressure is applied to the system when the speed is v and the potential head is h, and that p' static pressure is applied when the speed has changed to v' and the static head is h', Bernouilli's theorem, applied to the system, becomes

$$\frac{p_o}{\rho g} + \frac{v^2}{2g} + h = \frac{p'}{\rho g} + \frac{v'^2}{2g} + h'$$

When this result is applied to the portion of water in contact with the cap with the initial speed v = 0, the following equation applies

$$p_o = p' + \frac{v'^2\rho}{2} + (h' - h)\rho g \qquad (2)$$

The variation of static head $(h' - h)\rho g$ is a negligible term in comparison with the other terms in Eq. (2), and it is possible to write

$$p_o = p' + \frac{v'^2\rho}{2}$$

Equation (1) becomes

$$m\frac{d^2x}{dt^2} = p_o S - \left(k + \frac{\rho}{2} S\right)\left(\frac{dx}{dt}\right)^2 \qquad (3)$$

or

$$\left(\frac{dx}{dt} \right)^2 = \left(\frac{-m}{k + \frac{\rho}{2} S} \right) \left(\frac{d^2x}{dt^2} \right) + \frac{p_o S}{k + \frac{\rho}{2} S} \tag{4}$$

This nonlinear differential equation can be solved for

$$\left(\frac{dx}{dt} \right)^2 = f(x)$$

The general solution of Eq.(4) is

$$\left(\frac{dx}{dt} \right)^2 = Ae^{px} + B \tag{5}$$

After derivation we get

$$2 \left(\frac{dx}{dt} \right) \frac{d^2x}{dt^2} = Ape^{px} \cdot \frac{dx}{dt}$$

and

$$\frac{d^2x}{dt^2} = \frac{A}{2} pe^{px}$$

Equation (4) becomes

$$Ae^{px} + B = - \frac{m}{k + \frac{\rho}{2} S} \frac{A}{2} pe^{px} + \frac{p_o S}{K + \frac{\rho}{2} S} \tag{6}$$

$$B = \frac{p_o S}{k + \frac{\rho}{2} S}$$

and

$$Ae^{px} = \frac{mAp}{2\left(k + \frac{\rho}{2} S\right)} \quad e^{px}$$

$$p = - \frac{2k + \rho S}{m}$$

Initial conditions: for $x = 0$ $\quad \frac{dx}{dt} = 0$

Then, Eq. (6) becomes

$$0 = \frac{mAp}{2\left(k + \frac{\rho}{2} S\right)} + \frac{p_o S}{k + \frac{\rho}{2} S}$$

$$A = \frac{2Sp_o}{mp}$$

If (p) is replaced by its value, we get

$$A = - \frac{p_o S}{k + \frac{\rho}{2} S}$$

and Eq. (5), which represents the general solution of Eq. (3), can be written

$$\left(\frac{dx}{dt}\right)^2 = - \frac{p_o S}{k + \frac{\rho}{2} S} \exp\left(- \frac{2k + \rho S}{m} x\right) + \frac{p_o S}{k + \frac{\rho}{2} S}$$

and finally,

$$\left(\frac{dx}{dt}\right)^2 = \frac{p_o S}{k + \frac{\rho}{2} S} \left[1 - \exp\left(-\frac{2k + \rho S}{m} x\right)\right] \quad (7)$$

which is the equation of motion for the propulsion phase.

Conclusion:

$$\text{for } x \to \infty \qquad \left(\frac{dx}{dt}\right)^2 \to \frac{p_o S}{k + \frac{\rho}{2} S}$$

which corresponds to the asymptotical speed limit. But

$$\left(\frac{dx}{dt}\right)^2 \quad \text{for } x \nearrow \infty = \frac{p_o}{\left(\frac{k}{S} + \frac{\rho}{2}\right)}$$

$$\left(\frac{dx}{dt}\right)^2_{\infty} \quad \text{is a function of } S$$

We see that for $S \nearrow \infty \left(\frac{dx}{dt}\right)^2 \to \frac{2p_o}{\rho}$
which is Torricelli's theorem

The theoretical S should be as large as possible; however, one should keep in mind that k increases with S.

4. DYNAMICS OF THE PENETRATION PHASE

To make the calculus simple, we assume the friction of f dynes/cm^2 to be constant at any given place, although f may vary within wide limits according to the character of the sediments. If the frictional resistance to a tube within

the diameter ϕ is denoted by r dynes/cm, we have

$$r = f\pi\phi$$

Then the equation of motion for the tube and its cap, when they are going down into the bottom, is

$$m \frac{d^2x}{dt^2} = mg \left(1 - \frac{1}{d}\right) - k \left(\frac{dx}{dt}\right)^2 - rx \tag{8}$$

x = the depth of penetration

Equation (8) can be written

$$\left(\frac{dx}{dt}\right)^2 = - \frac{m}{k} \cdot \frac{d^2x}{dt^2} - \frac{r}{k} x + \frac{mg}{k} \left(1 - \frac{1}{d}\right) \tag{9}$$

The term $\frac{mg}{k} \left(1 - \frac{1}{d}\right)$ will be very small in comparison with the other terms of Eq. (9). Therefore, we shall neglect it and consider only the equation

$$\left(\frac{dx}{dt}\right)^2 = - \frac{m}{k} \cdot \frac{d^2x}{dt^2} - \frac{r}{k} x \tag{10}$$

This nonlinear differential equation can be solved for

$$\left(\frac{dx}{dt}\right)^2 = f(x)$$

The general solution of this equation is

$$\left(\frac{dx}{dt}\right)^2 = Ae^{px} + Bx + C \tag{11}$$

After derivation we get

$$\frac{d^2x}{dt^2} = \frac{A}{2} pe^{px} + \frac{B}{2} \qquad (12)$$

Replacing the values of Eqs. (11) and (12) in Eq. (10), we obtain

$$Ae^{px} + Bx + C = -\frac{mAp}{2k} e^{px} - \frac{mB}{2k} - \frac{r}{k} x$$

By identification, we see

$$Ae^{px} = -\frac{mAp}{2k} e^{px}$$

$$p = -\frac{2k}{m}$$

$$B = -\frac{r}{k}$$

$$C = -\frac{mB}{2k} = \frac{mr}{2k^2}$$

Equation (11) becomes

$$\left(\frac{dx}{dt}\right)^2 = Ae^{px} - \frac{r}{k} x + \frac{mr}{2k^2} \qquad (13)$$

Initial conditions: for $x = 0$ and $v = v_o$

$$v_o^2 = A + \frac{mr}{2k^2}$$

and

$$A = v_o^2 - \frac{mr}{2k^2}$$

Equation (13) then becomes

$$\left(\frac{dx}{dt}\right)^2 = v_o^2 - \frac{mr}{2k^2} e^{-\frac{2k}{m}x} - \frac{r}{k}x + \frac{mr}{2k^2} \qquad (14)$$

which is the equation of motion for the penetration phase

5. NUMERICAL APPLICATION

A prototype of the mechanical system has been designed and will be described later in the paper. The behaviour of the system under the external pressure found at 2500 m depth (i.e., at $\approx$ 250 kg/cm^2 pressure) is studied here.

5.1 Characteristics of Equipment

Length of tube	$\approx$	400	cm
Inside diameter of tube	$\approx$	7.5	cm
Outside diameter of tube	$\approx$	9.0	cm
Inside section of tube	$\approx$	40.0	cm^2
Outside diameter of nose	$\approx$	11.5	cm
Mass of the tube	$\approx$	30,000	gm
Mass of cap	$\approx$	100	gm
Mass of piston	$\approx$	90,000	gm

5.2 Drag coefficient of the equipment

The hydrodynamic resistance of the tube moving in the fluid is

$$R = \frac{CS_1\rho}{2} v^2$$

We shall write

$$k = \frac{CS_1\rho}{2} \quad \text{and} \quad R = kv^2$$

C = a geometrical coefficient of drag depending on the Reynolds number

S_1 = a section of the solid in a plane perpendicular to the displacement line (in this case, the section of the nose bit)

ρ = the specific mass of water

The expected speed of the solid in water V is $\approx 10^4$ cm/sec and the Reynolds number N is Vd/ν , where d is the outside diameter of the nose (11.5 cm) and ν is the dynamic viscosity coefficient of fluid ($\nu = \eta/\rho$ = static viscosity of fluid/specific mass of fluid).

$$\nu \approx \frac{10^{-2}}{1} \quad \text{for water}$$

$$N \approx 10^7$$

For $N = 10^7 \rightarrow C \approx 0.3$ (from Fig. 2, part cd of the curve)

$$k = \frac{CS_1\rho}{2}$$

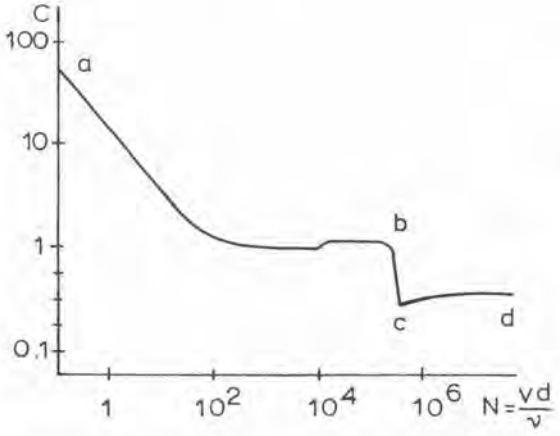

Fig. 2 Variation of Drag Coefficient versus Reynolds Number

We shall consider the tube as a solid bar; in this way, we exaggerate considerably the coefficient of drag, but we shall assume that this compensates for the neglected internal friction in the tube.

S = Section of nose bit 95 cm^2

C = 0.3

ρ = 1 gm/cm^3

$k \approx 15$ gm/cm

5.3 Propulsion Period of Motion

The following is derived from Eq. (7), the equation of motion during the propulsion period. The ambient pressure at 2500 m depth is $\approx 250 \times 981,000$ ($\approx 2.5 \times 10^{-8}$) dynes/$cm^2$.

S = 40 cm^2

k = 15 gm/cm

ρ = 1 gm/cm^3

$$\frac{p_o S}{k + \frac{\rho}{2} S} = 2.8 \times 10^8 \text{ (cm/sec)}^2$$

$$\frac{2k + \rho S}{m} = 2.33 \times 10^{-3} \text{ cm}^{-1}$$

The asymptotic speed will be $\sqrt{2.8 \times 10^4}$ cm/sec or 167 m/sec.

Since the mass of the piston is approximately three times that of the tube assembly, the total motion of the tube, during the propulsion period, should be about 3/4 the total length of the tube, i.e., 3 metres. (See Section 2).

For x = 300 cm, and with all terms replaced by calculated values, Eq.(7) becomes

$$\left(\frac{dx}{dt}\right)^2 = 2.8 \times 10^8 \left(1 - e^{-0.7}\right)$$

$$= 2.8 \times 10^8 \left(1 - 0.497\right)$$

$$\frac{dx}{dt} = 1.18 \times 10^4 \text{ cm/sec}$$

$$= 118 \text{ m/sec}$$

We see that this sytem will not have the maximum efficiency. Only 118/167 or 70% of the maximum speed will be obtained during the propulsion phase. To make the system more efficient, the masses of the cap and tube assembly should be smaller and the tube length much longer. For a tube 10 m long, 90% of the speed limit will be produced during the propulsion period.

5.4 Penetration Period of Motion

The equation of motion during the penetration period was given by Eq.(14). We have seen that $r = f\pi\not{\phi}$, where $\not{\phi}$ is the external diameter of the nosebit. For low speed corers, the friction resistance of the sediments is generally considered to be about 4×10^4 dynes/cm^2.

In the case of high speed corers, most of the friction occurs along the outside and inside diameters of the nosebit, which are respectively larger and smaller than the coring tube itself. The sediments inside and outside the coring tube are frozen during the penetration process and very little friction occurs between

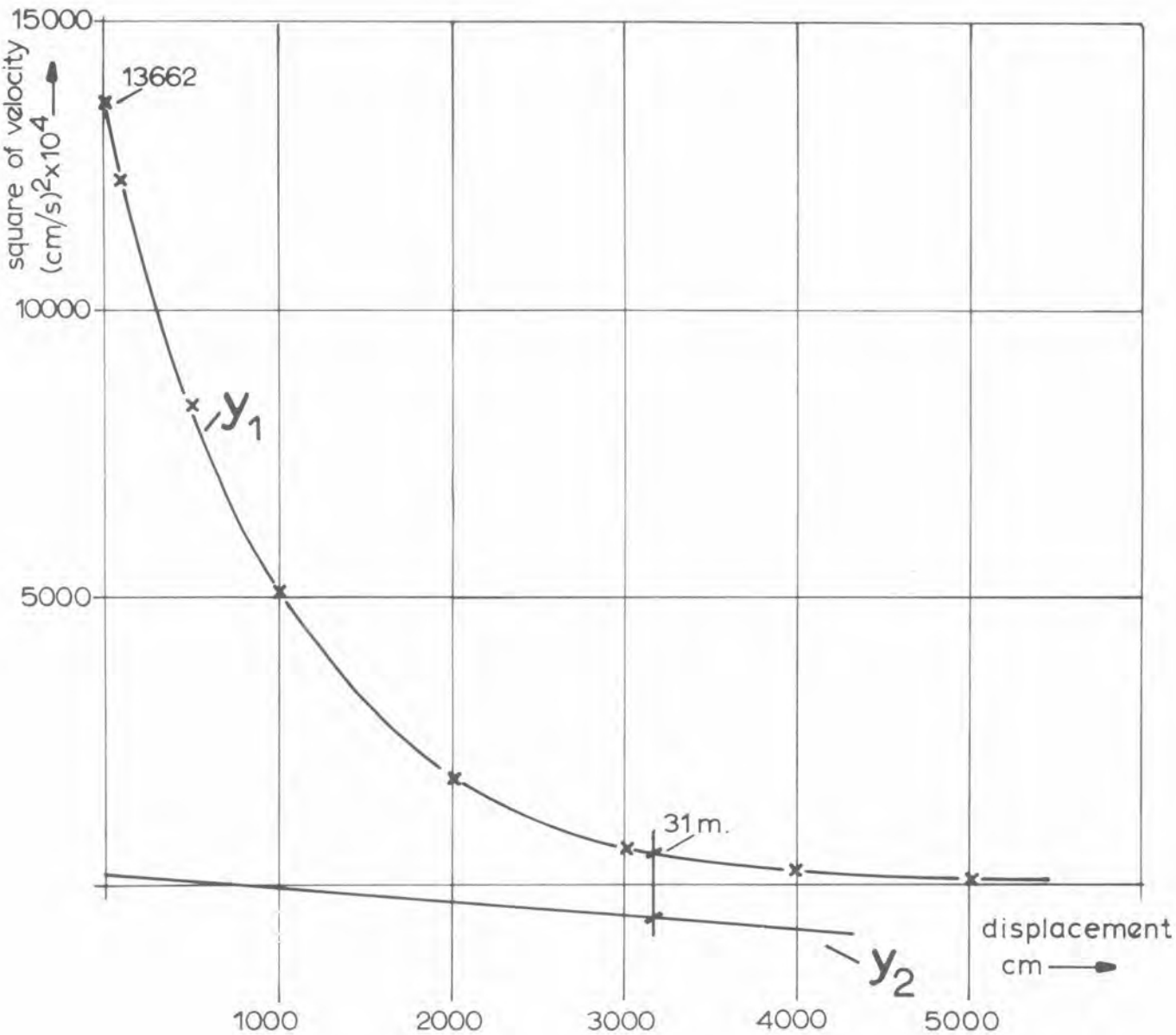

Fig. 3 Speed versus Penetration for the Full Scale Model

the coring tube and the surrounding medium. Therefore, f has been assumed to be around 10^3 dynes/cm^2 and

$$r = 10^3 \times \pi \times 11.5$$

$$= 3.6 \times 10^4 \text{ dynes/cm}$$

The various parameters of Eq. (14) can be calculated, with

$$v_o^2 = 1.4 \times 10^8 \text{ (cm/sec)}^2$$

$$\frac{mr}{2k^2} = 2 \times 10^6 \text{ (cm/sec)}^2$$

$$-\frac{2k}{m} = 10^{-3} \text{ cm}^{-1}$$

$$\frac{r}{k} = 0.24 \times 10^4 \text{ cm/sec}^2$$

the equation becomes

$$\left(\frac{dx}{dt}\right)^2 = 10^4 (13,800\, e^{-10^{-3}x} - 0.24x + 200) \qquad (15)$$

which can be written

$$y = y_1 + y_2 = 10^4 \cdot 13,800\, e^{-10^{-3}x} + 10^4 (-0.24x + 200)$$

Figure 3 presents a plot of speed versus penetration for the full scale model; the functions of y_1 and y_2 are taken therefrom and presented in the tables which follow.

TABLE 1 - Functions of y_1	
x	$y_1 \times 10^{-4}$
cm	$(\frac{cm}{s})^2$
10	13662
100	12489
400	9246
500	8376
1000	5078
1100	4595
1200	4153
1500	3077
2000	1863
3000	687
4000	252
5000	93

TABLE 2 - Functions of y_2	
x	$y_2 \times 10^{-4}$
cm	$(\frac{cm}{s})^2$
0	200
400	104
834	0

An inspection of Fig. 3 shows a corer speed of ≈ 0 at a penetration of about 31 metres. However, to avoid deformation of the core, we must stop the tube when it has penetrated approximately 4 metres and still has a high velocity: i.e., for x = 4m, $v_4 = 96.5$ m/sec. Special arresting chains have been designed to stop the tube; these will be discussed in a later section.

6. COMPARISON OF SPEEDS OF PISTON AND TUBE DURING PROPULSION PERIOD

Equation (7) is the general equation of motion during the propulsion period. If we suppose now that the drag coefficient of the pision is identical to that of the tube, the equation of motion for the piston during the propulsion period will be

$$\left(\frac{dx}{dt}\right)^2 = \frac{p_o S}{k + \frac{\rho}{2} S} \left[1 - \exp\left(-\frac{2k + \rho S}{M} x\right)\right] \tag{16}$$

All terms of this equation are the same as those in Eq. (7) except that the mass of the piston M is now three times that of the combined mass of the tube and cap m. By analogy to an RC electrical circuit

$$\frac{M}{2k + \rho S} \quad \text{and} \quad \frac{m}{2k + \rho S}$$

will be called the "travel constants" of each respective motion (the "time constant" of an RC electrical circuit).

From Eq. (7), for $x = \frac{m}{2k + \rho S}$

$$\left(\frac{dx}{dt}\right)^2 = \frac{p_o S}{k + \frac{\rho}{2} S} \left(1 - e^{-1}\right)$$

$$= 63\% \text{ (Speed Limit)}^2$$

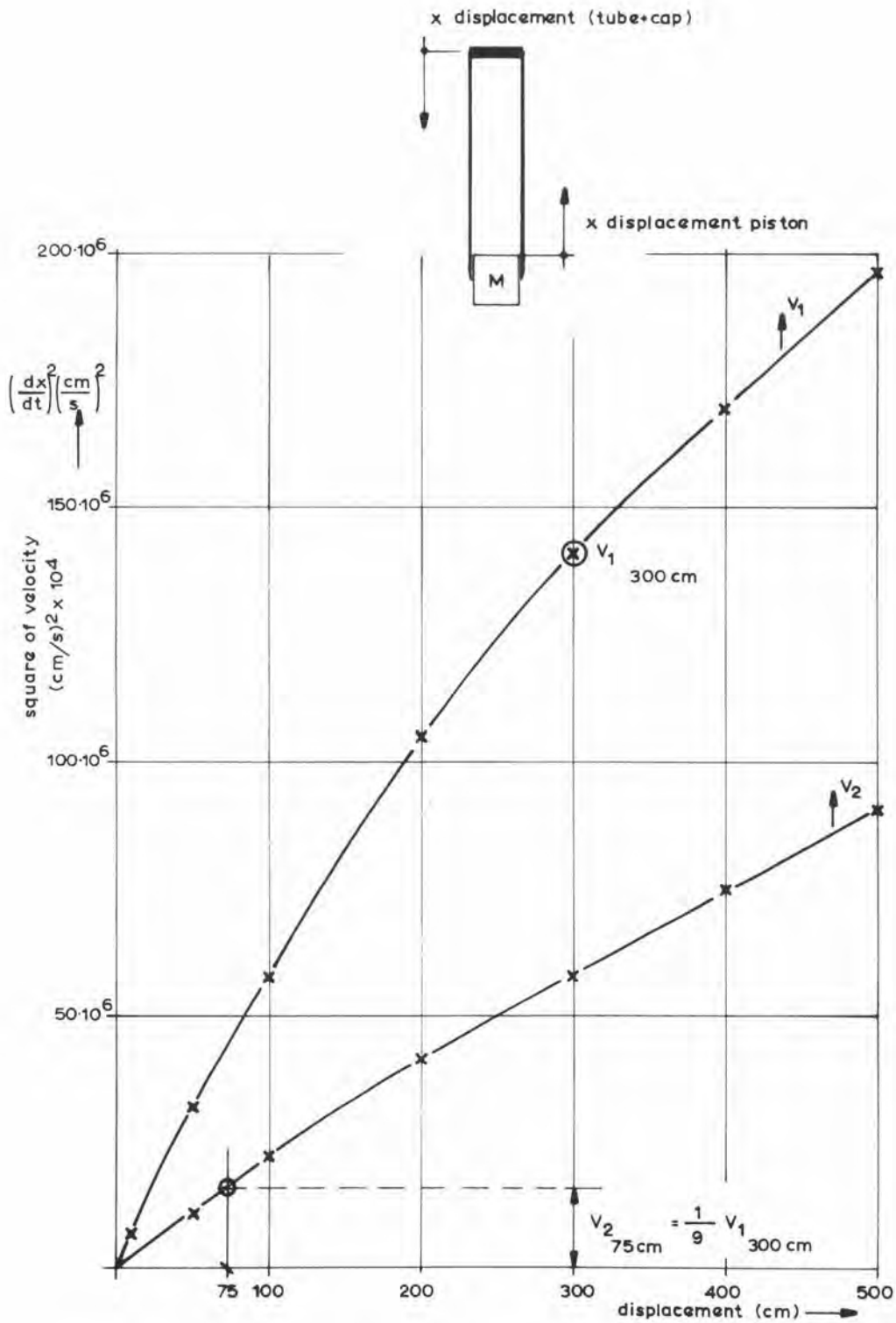

Fig. 4 Comparative Speeds of the Piston and the Tube During the Propulsion Period of Motion

From Eq. (16), for $x = \frac{M}{2k + \rho S}$

$$\left(\frac{dx}{dt} \right)^2 = \frac{p_o S}{k + \frac{\rho}{2} S} \left(1 - e^{-1} \right)$$

$$= 63\% \text{ (speed limit)}^2$$

The "travel constant" of the piston is then 3 times the "travel constant" of the tube.

A comparison of the squared piston speed V_1 and the squared tube speed V_2 has been computed from the equation of motion (Eq. (16)) for each and plotted in Fig. 4.

Table 3 presents some selected values taken from Fig. 4, for both V_1 and V_2.

TABLE 3

x	$V_1 = f(x)$	$V_2 = f(x)$
cm	$10^{-6}(\text{cm/sec})^2$	$10^{-6}(\text{cm/sec})^2$
0	0	0
10	5.6	
50	31.6	10.9
100	57.4	21.5
200	105.0	41.4
300	140.8	57.4
400	169.4	74.8
500	195.7	90.4

We shall assume that, during the propulsion period, the mechanical system is submitted to external forces only. This assumption is not fully correct because various friction forces, developed during the motion, are not negligible. However, to have some idea on the displacement of the piston or the tube, we shall assume the conservation of kinetic moments; hence, we can write

$$MV = mv \tag{17}$$

where

V = instantaneous speed of the piston

v = instantaneous speed of the tube

M = mass of the piston

m = mass of the tube .

Equation (17) can be written

$$\left(\frac{v}{V}\right)^2 = \left(\frac{M}{m}\right)^2$$

$$\frac{V_1}{V_2} = \left(\frac{M}{m}\right)^2 = 9 \text{ for the full scale prototype}$$

Reading from Fig. 4, for $x_{tube} = 300$ cm, $V_1 \approx 140.8 \times 10^6$ $(cm/sec)^2$ for $V_2 = \frac{140.8 \times 10^6}{9} = 16.5 \times 10^6$ $(cm/sec)^2$ then

$$x_{piston} = 75 \text{ cm}$$

instead of 1 m previously assumed in the calculations of Section 4.

We then see that

$$x = \frac{1M}{M + m},$$

which is the travel distance of the tube compared to its total length is about correct

7. MODEL EXPERIMENTS IN HIGH PRESSURE CHAMBER

Figure 5 is a schematic drawing of the model.

Length of tube	45 cm
Length of piston	30 cm
Internal tube diameter	4.4 cm
External tube diameter	5.0 cm

A brass shearing pin (3mm diam.) holds the piston rigid to the tube until the pressure reaches 38 kg/cm^2.

Figure 6 shows the arrangement of the pressure chamber. To compensate the pressure variation when the mechanical system tube piston implodes, a cushion of compressed air is used on the top of the water. An air bottle, connected to the pressure chamber by an "aqualung" tube, supplies the compressed air.

Because the flow of air from the bottle does not match the speed of the implosion, there will be a pressure decrease when the implosion occurs; consequently, the motion of both tube and piston is somewhat slowed down.

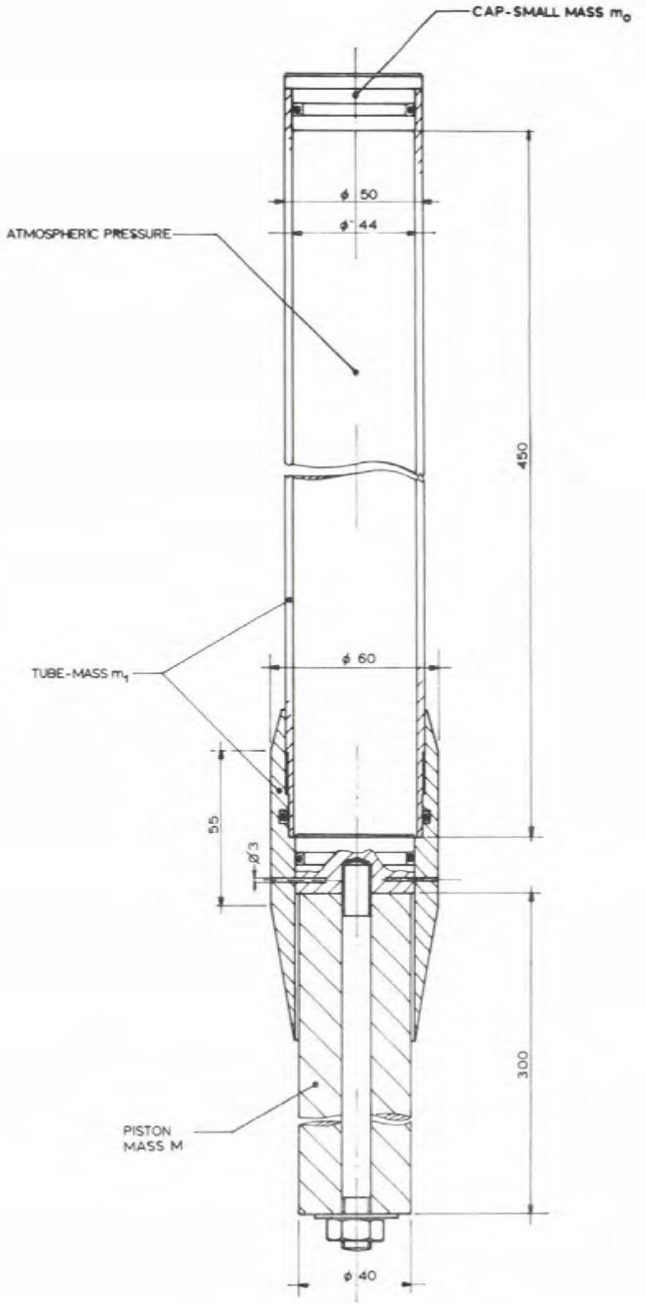

Fig. 5 The Model: Mechanical Characteristics

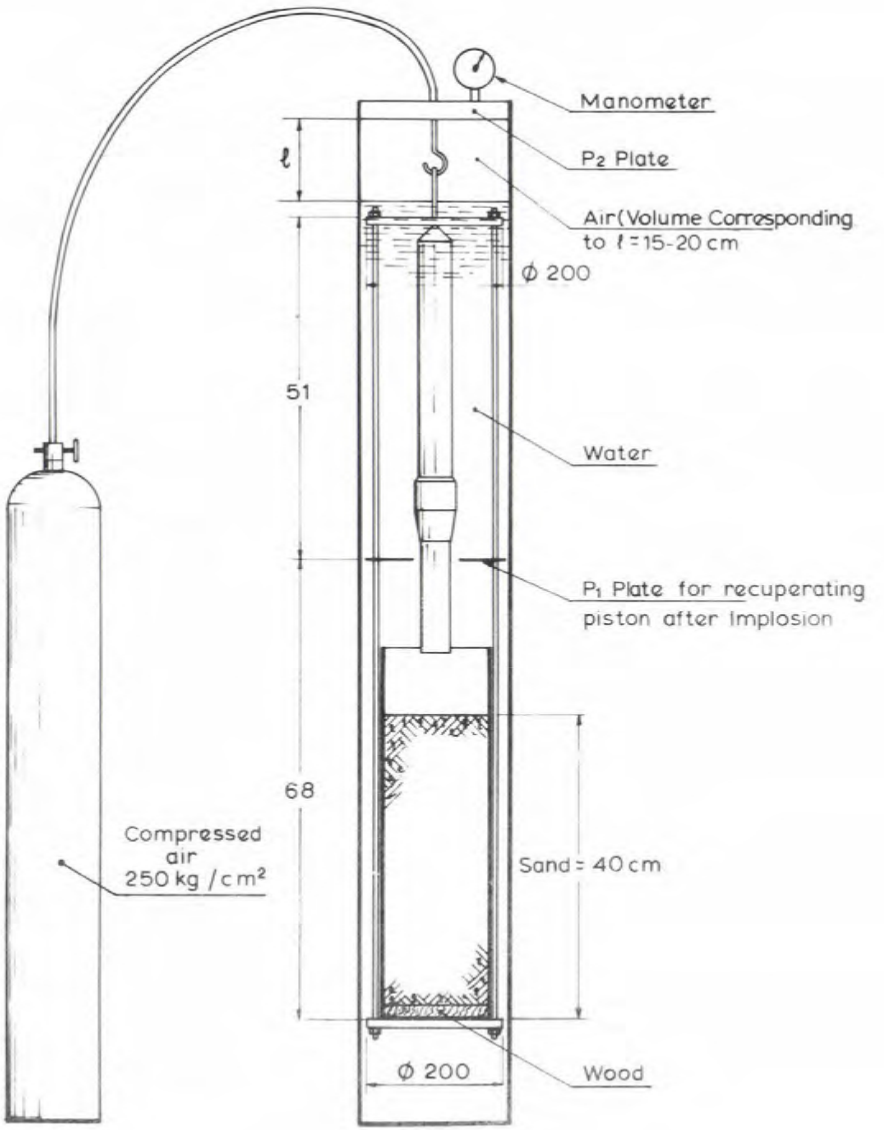

Fig. 6 Model Studies in Pressure Chamber

7.1 Propulsion Period of Motion

The following values may be assigned to the equation of motion (Eq. (7)). The inside section of the tube is about 15 cm^2

p_o = 38 x 981,000 dynes/cm^2

S = 15 cm^2

k = 10(the drag coefficient is probably exaggerated in comparison with the full scale model)

m = Mass of tube = 2000 gm

M = Mass of piston = 4000 gm

$$\frac{p_o S}{k + \frac{\rho}{2} S} = 32 \times 10^6 \ (cm/sec)^2$$

$$\frac{2k + \rho S}{m} = 1.75 \times 10^2 \ cm^{-1}$$

Since the mass of the piston is twice that of the tube, the displacement of the piston will be roughly half that of the tube during propulsion. The total motion of the tube will then be $\frac{40 \times 2}{3}$ cm $\approx$ 26 cm (See Section 2). Therefore,

$$\exp\left(-\frac{2k + \rho S}{m} x\right)$$

for

$$x = 26 \text{ cm}$$

becomes

$$e^{-0.45} = 0.638$$

and

$$\left(\frac{dx}{dt}\right)^2 = 11.5 \times 10^6 \text{ (cm/sec)}^2$$

$$v = \frac{dx}{dt}$$

$$v = 34 \text{ m/sec}$$

The speed limit would be

$$v_{limit} = \sqrt{32} \times 10^3 \text{ cm/sec}$$

$$= 56 \text{ m/sec}$$

It can be seen that maximum efficiency is not obtained by the tube length selected for the model.

7.2 Penetration Period of Motion

The equation of motion (Eq. (14)) was used for the calculations that follow. Since the penetration medium is sand, we shall assume the frictional resistance r to be 10 times larger than the value previously taken. Then

$$r = 3.6 \times 10^5$$

$$\frac{mr}{2k^2} = 3.6 \times 10^6 \text{ (cm/sec)}^2$$

$$v_o^2 - \frac{mr}{2k^2} = 7.9 \times 10^6 \text{ (cm/sec)}^2$$

$$-\frac{2k}{m} = -1.0 \times 10^{-2} \text{ cm}^{-1}$$

$$\frac{r}{k} = 3.6 \times 10^{4} \text{ cm/sec}^2$$

The equation of motion is then

$$\left(\frac{dx}{dt}\right)^2 = 7.9 \cdot 10^6 e^{1 \cdot 10^{-2}x} - 3.6 \cdot 10^4 x + 3.6 \cdot 10^6$$

For x = 40 cm thickness of sand in the pressure chamber

$$\left(\frac{dx}{dt}\right)^2 = 7.5 \times 10^6 \text{ (cm/sec)}^2$$

$$v = \frac{dx}{dt} = 2.7 \times 10^3 \text{ cm/sec}$$

$$= 27 \text{ m/sec}$$

It is obvious that the tube speed is high even after 40 cm of penetration in sand.

7.3 Tests in the Pressure Chamber

About 50 qualitative model tests have been made in the pressure chamber. Of these, 5 failed because of mechanical troubles, but some 45 good results were obtained.

For most tests, the release pressure was 35 to 38 kg/cm^2. At this pressure, on each occasion of proper function, the tube penetrated the 40 cm of sand. On the first few trials, the tube also penetrated the 15 mm pinewood bottom and the 0.3 mm steel container. This demonstrated the force potential; however, to eliminate further damage to the system, a thicker piece of wood

was placed in the bottom. Figures 7 and 8 are photographs of the model and Fig. 7 demonstrates the penetration of the wood bottom and the cores taken therefrom.

Several tests were made at lower release pressures (10 - 15 kg/cm^2), and 90% of the sand thickness was penetrated at these pressures.

The length of the core was always equal to the penetration distance; this seems to prove that, for this depth of penetration at least, no compaction effects occur in the core.

Quantitative tests were not possible under the present conditions; however, some measurements are planned for the near future. These should improve our knowledge of the dynamics of the system.

8. FULL SCALE PROTOTYPE HYDROSTATIC CORER

8.1 Functional Parts (Figure 9)

The prototype corer is composed of three main functional parts:

(1) The Cap

(2) The Tube-Nose Assembly

(3) The Piston Assembly

8.1.1 The Cap is mounted to the upper end of the tube sealing it watertight with "O" rings. It can move vertically upwards and out of the tube, but it is prevented from downward movement, or into the tube, by a flange.

8.1.2 The Tube-Nose is an aluminum tube (4 m long with internal and external diameters 75 and 90 mm respectively) fitted with a hard steel nose to provide for penetration. The nose is fitted with "O" rings to make the lower part of the tube

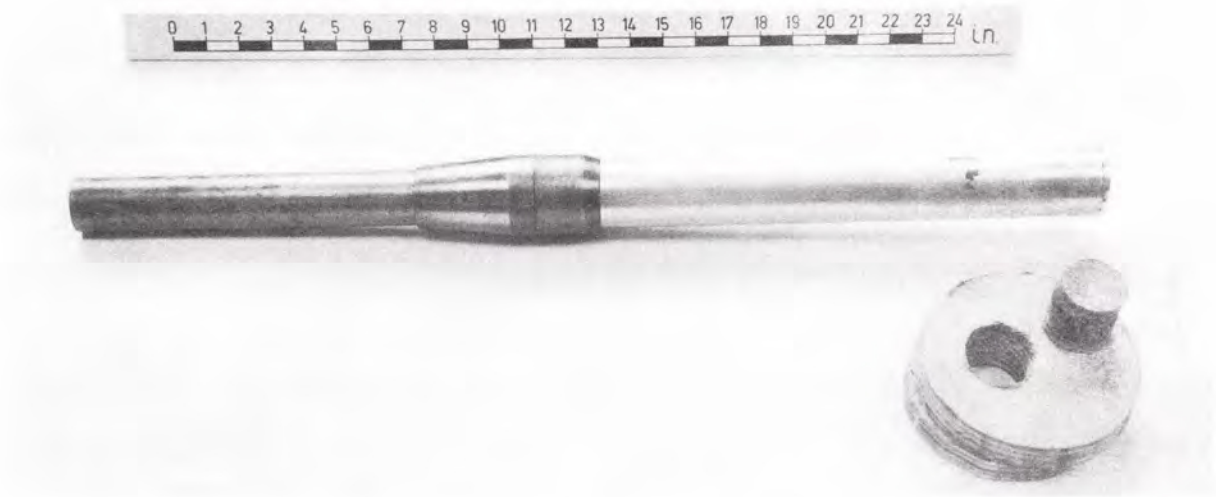

Fig. 7 The Model Mounted - with a Release Pressure of 38 kg/cm^2.
The Corer has Perforated 5 cm of Plywood.

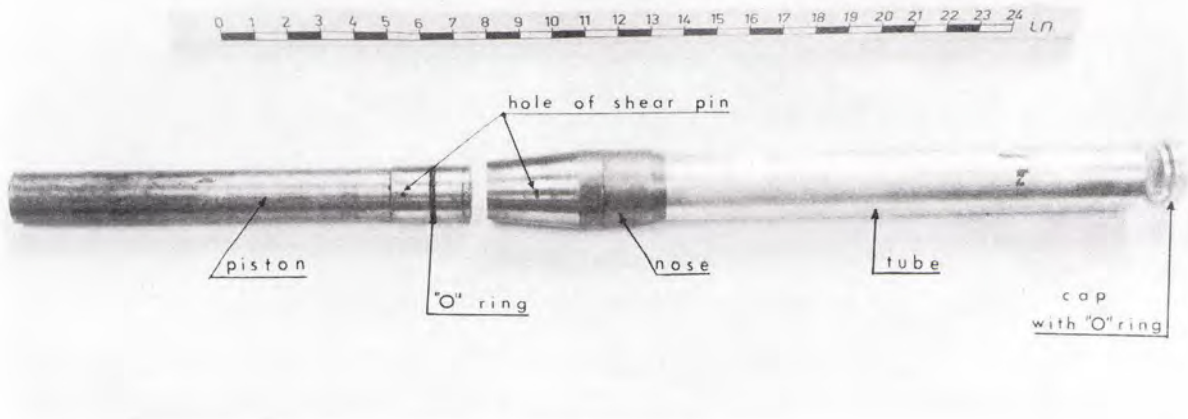

Fig. 8 Exploded View of the Model

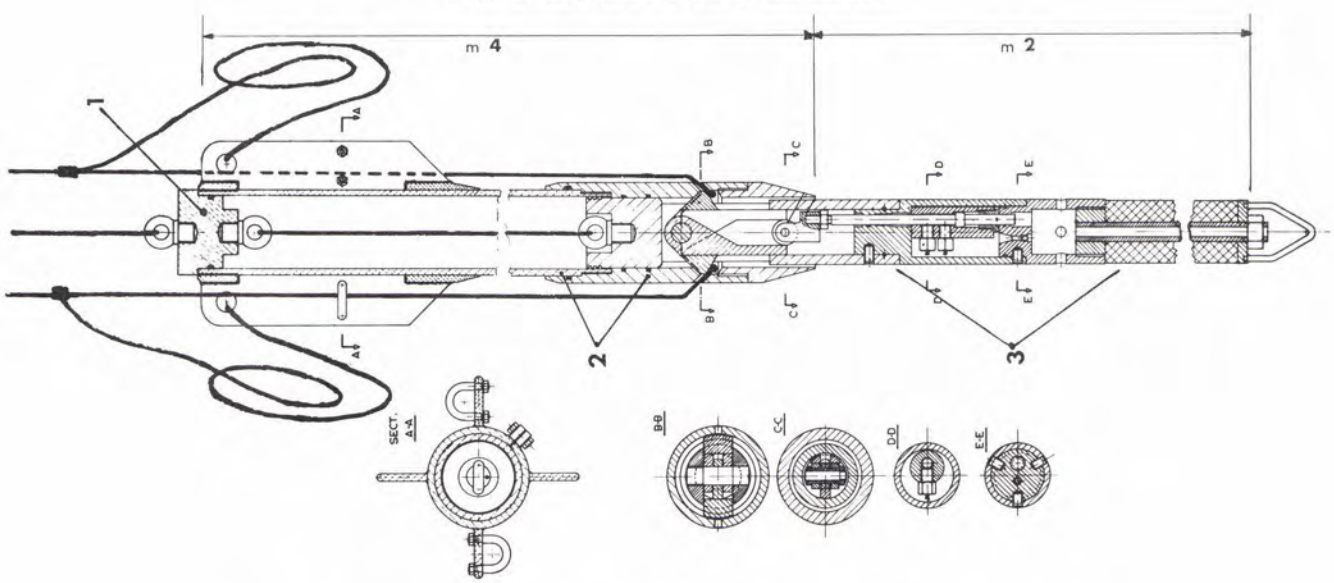

Fig. 9 Mechanical Parts of the Full Scale Hydrostatic Corer - Drawing

watertight on the piston. The weight of the assembly is approximately 30 kg.

8.1.3 The Piston is a cylindrical body, the upper part of which is hollow and slotted. A mechanical device, consisting of two locking jaws and associated locking-releasing mechanism, is fitted into the hollow core in the upper part of the piston. When in locked position, the jaws protrude through the slots in the piston and lock it to the nose section of the tube; when released, the jaws collapse into the piston leaving it free to move in the tube. Also associated with the piston is a switch system with a mercury battery (shown in Fig. 10). When the corer is lowered, the switch case is suspended from the nose of the piston with a lead weight to make first contact with the bottom. When this occurs, small CONAX charges in the piston explode to set in motion the unlocking action and to liberate the piston from the tube

The apparatus also has a cable tying-up system; each cable has a very definite role before and after the functioning of the apparatus at the bottom. This is shown in the next section.

8.2 Functional Coring Steps

Figure 10 demonstrates the various steps performed during one complete coring operation.

Position 1: The apparatus approaches the bottom, the mercury switch has not yet made contact.

Position 2: The switch makes contact with the bottom; this fires an explosive CONAX charge, which sets in motion the piston releasing device freeing the piston from the tube.

Position 3: The liberated piston begins to ascend and the tube begins to accelerate

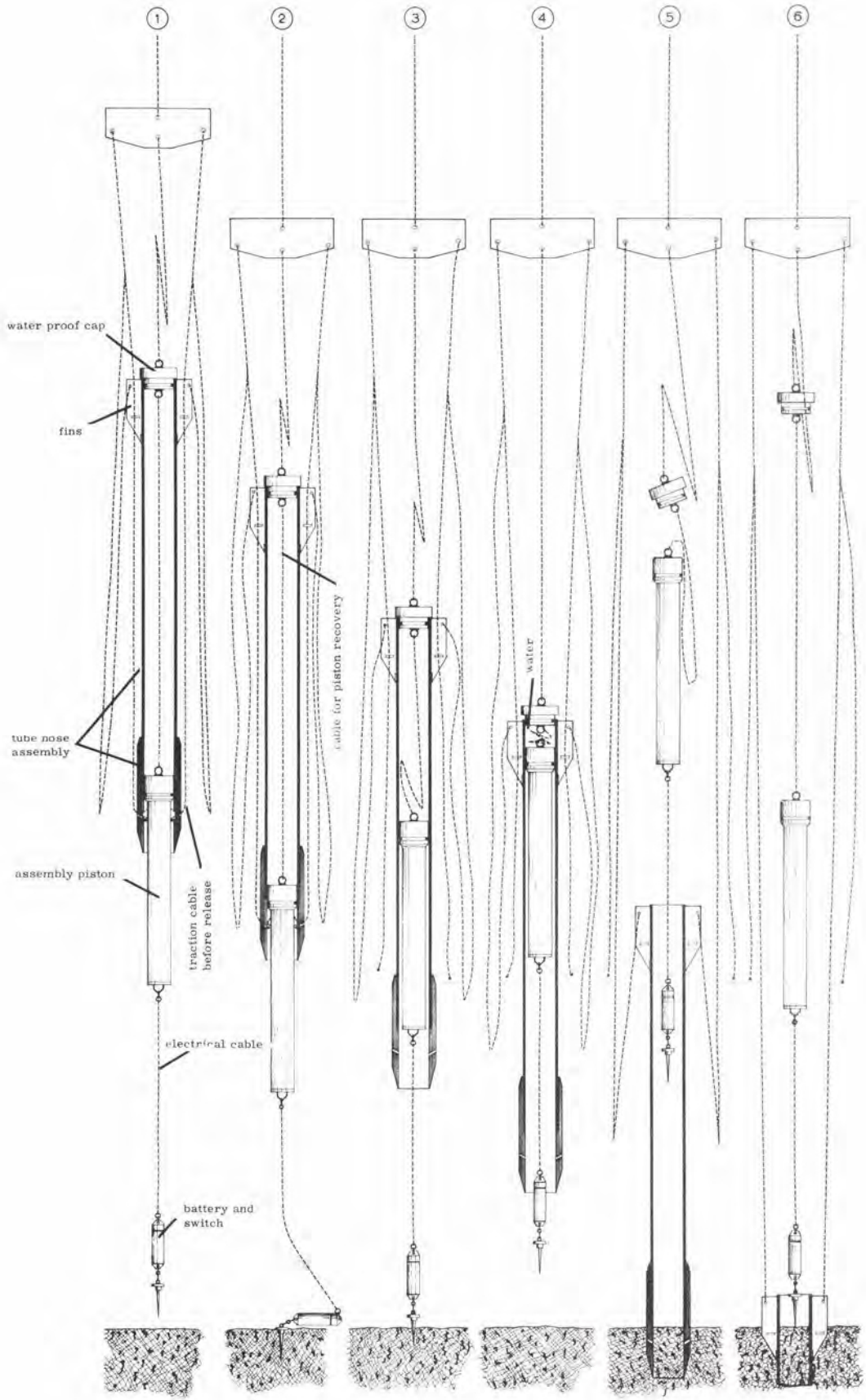

Fig. 10 Hydrostatic Corer: Principle

downward. The two traction cables are released when the piston begins to move; as the tube moves downward these cables play out through two guiding rings in the tube fins.

Position 4: The piston, which has let a small amount of water into the tube (the absolute watertightness is no longer ensured when the piston moves in the tube), reaches the end of its course. Since the air in the tube is compressed to a pressure equal to the external pressure (i.e., internal and external forces are equal), the movement of the heavy piston separates the lightweight cap from the relatively heavy tube.

Position 5: The tube, moving at high speed, begins penetrating the sediments.

Position 6: The tube penetrates the sediments. Its downward motion is stopped by arresting cables, which are also used to extract the corer with its core. The cap, piston, and switch are attached in series to a cable and are retrieved with the corer.

8.3 Illustrations

Figure 11 shows the lower part assembly of the prototype with only two lead weights mounted. The battery and switch are usually located farther away from the end of the piston by means of a steel cable.

Figure 12 shows the nose and piston assembly and the two 3 mm holding cables in position.

Figure 13 shows the upper part of the corer with the 3 cables used for retrieving the coring tube and piston assembly. Note the two 3 mm holding cables connected to the recuperation cables.

Figure 14 shows the various mechanical parts of the piston assembly.

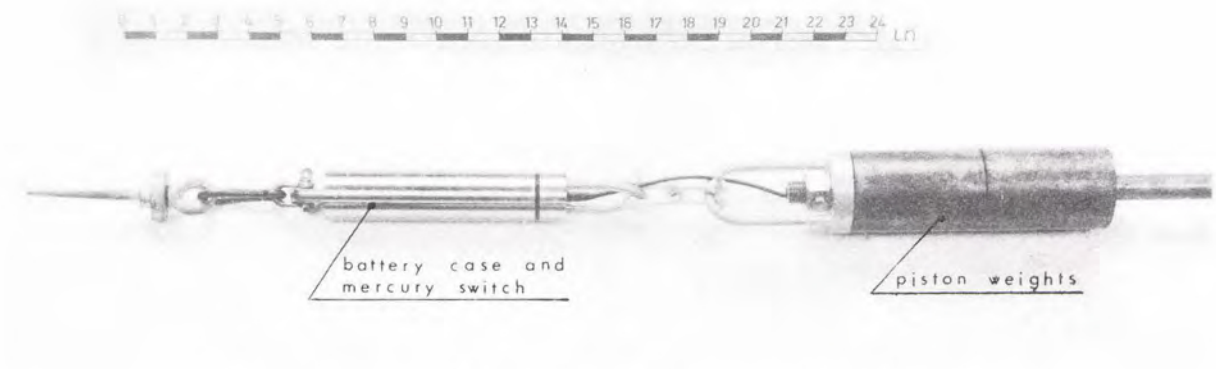

Fig. 11 The Lower Part Assembly of the Full Scale Prototype - Battery and Switch Case

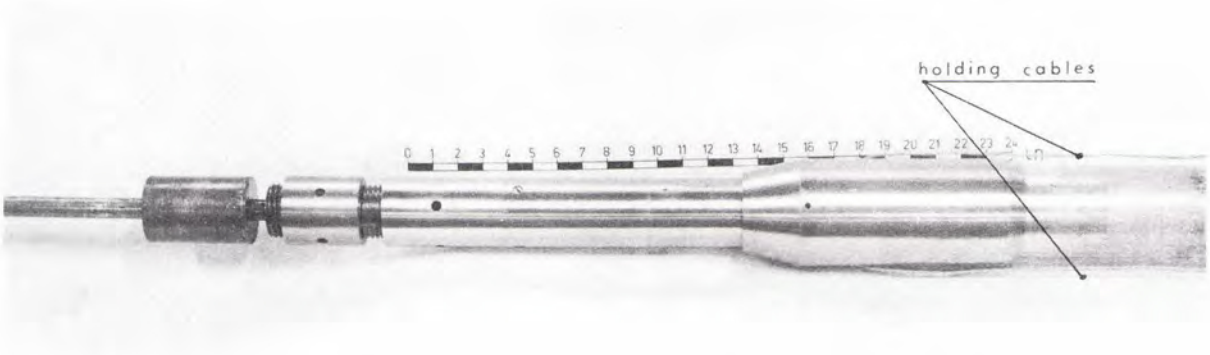

Fig. 12 The Nose and Piston Assembly with Holding Cables

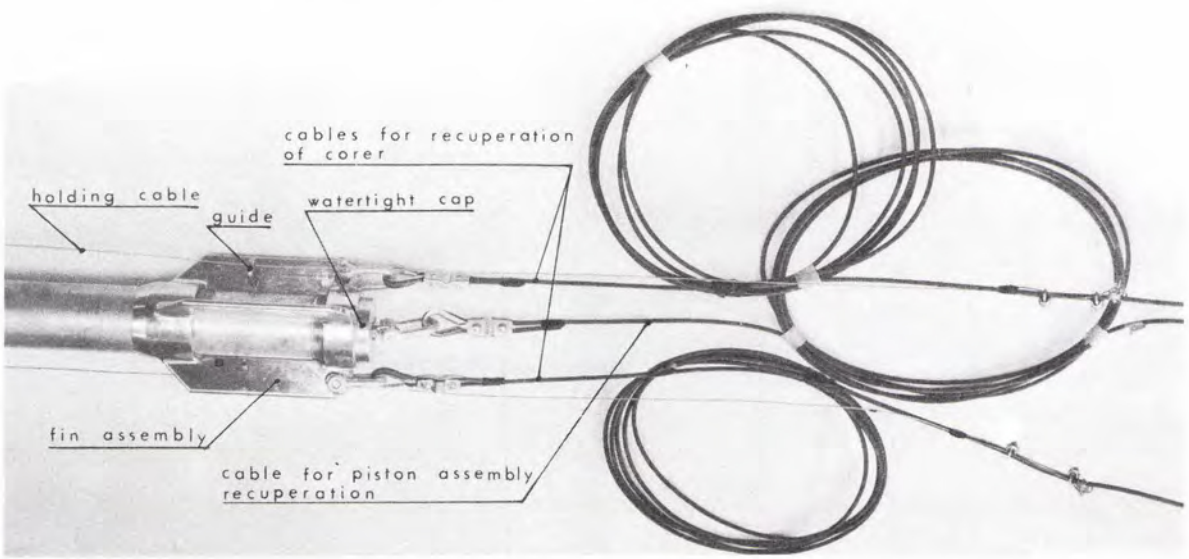

Fig. 13 Upper Part of Prototype with Tying-Up Cables

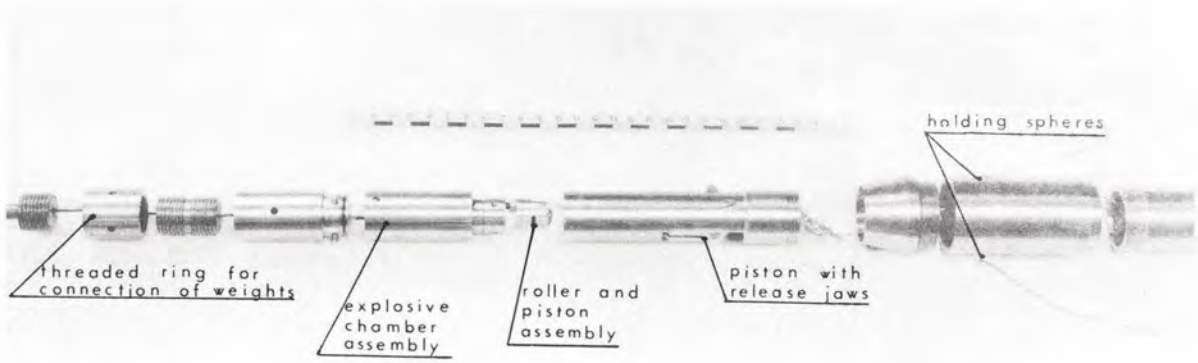

Fig. 14 Exploded View of Piston Assembly of Full Scale Prototype

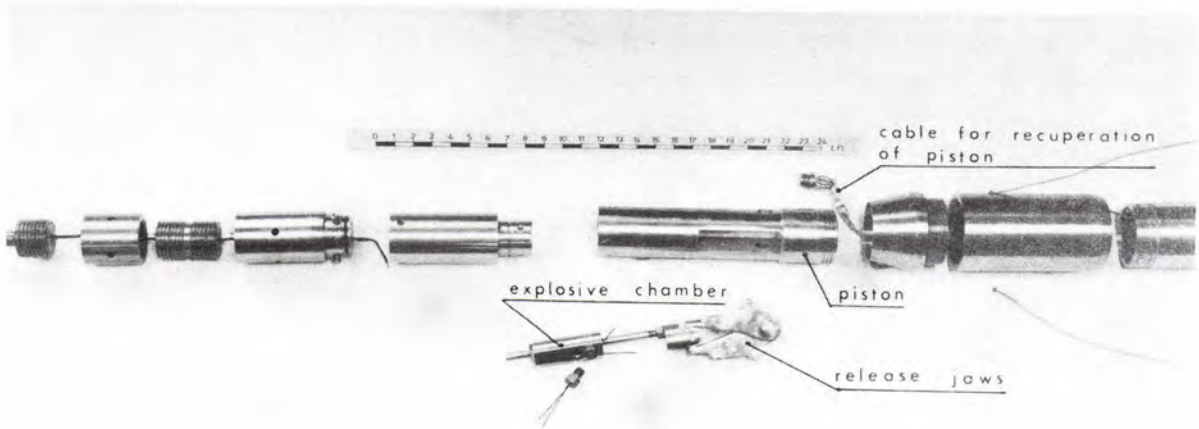

Fig. 15 Exploded View of Piston Assembly Showing Explosive Chamber

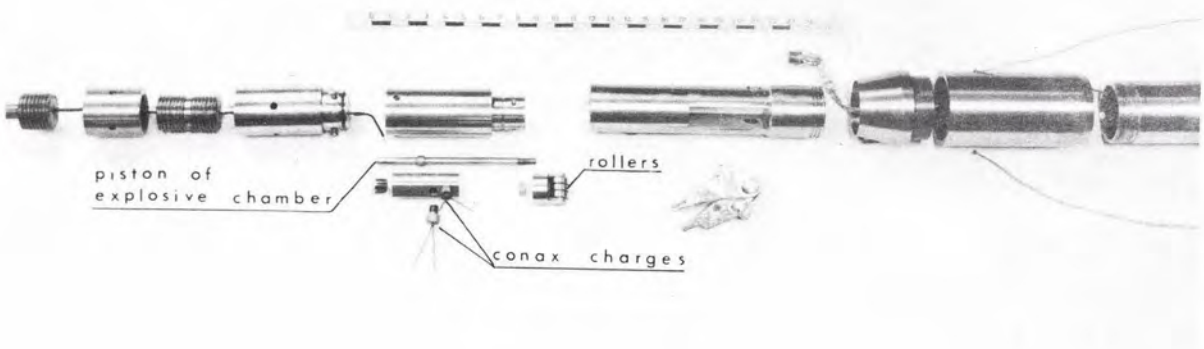

Fig. 16 Exploded View of Piston Assembly with Explosive Chamber Disassembled

Figure 15 shows the release system dismantled. The three rollers are represented in the locking position.

Figure 16 shows the various parts of the explosive chamber.

8.4 Core Catcher

A core catching system will eventually be installed on the nose of the tube; this will be a waterproof Delauze system with a nylon skirt.

9. CONCLUSIONS

This study has proved that long cores can be obtained with light equipment (150 kg) at great depths using hydrostatic pressure. The model experiments have shown that the energy involved makes the system particularly suited for coring sandy bottoms.

The length of cores obtained in the model experiments were all equal to the penetration depth of the corer, i.e., 40 cm.

10. REMARKS

The first prototype model has been completed and was tested at sea in January, (See Annex 1).

By authorization from the SUPREME ALLIED COMMANDER ATLANTIC, a patent has been filed on the principle of the tube accelerator.

11. ACKNOWLEDGEMENTS

The author wishes to express his gratitude for the help and guidance on the entire

project given by Drs. Dahme and Allan and Mr. Duykers and to Mr. Cortis for the design of both the model and the full scale prototype. He wishes also to acknowledge the contribution of Mr. Gehin, summer student, who made all the experiments with the model.

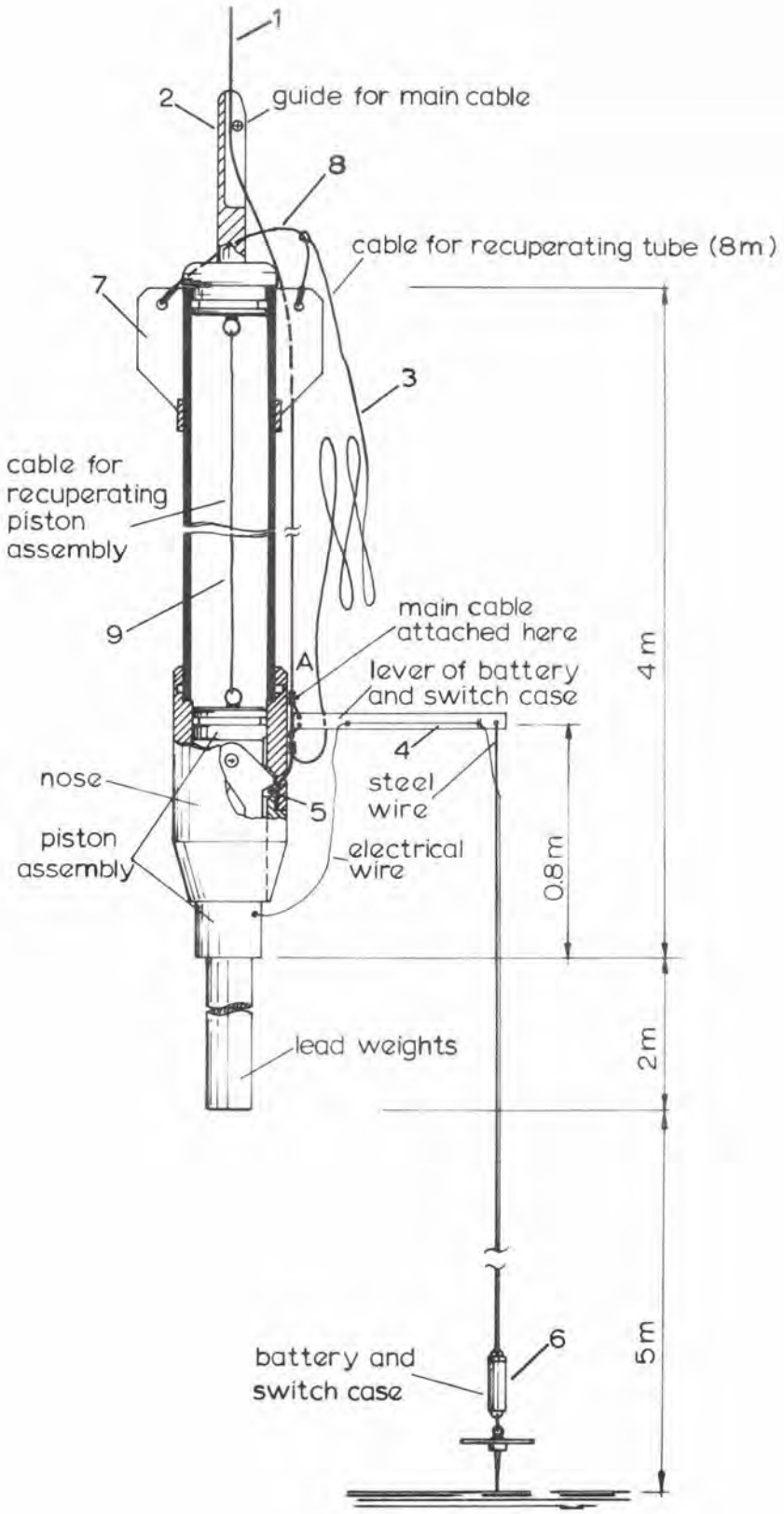

Fig. 17 Cable Arrangement During First Test at Sea

ANNEX 1

Recent Sea Tests

1. GENERAL

The full scale prototype was tested in shallow water during a cruise in January 1964 to prove the efficiency of the various mechanical parts of the system. Since very little hydrostatic pressure exists at shallow depth, the penetration into the sediments was small.

2. MODIFICATION ON THE CABLE ASSEMBLY

To avoid the problem of handling several cables, a few parts were modified in order to use only one cable for the recuperation of the tube and the piston assembly. Also, to make manoeuvres easier and to avoid the risk of the battery case hitting the coring tube, as was possible in the previous arrangement, the battery release system was suspended outside the corer by means of a small aluminum arm. This is shown on Fig. 17.

The main cable (1) goes through a guide (2) fixed on the cap. This guide keeps the system vertical. Cable (1) is attached in A to cable (3) for recuperation of the coring tube.

The main cable holds the system before implosion by means of spheres (5). The aluminum arm (4) holds the battery and switch case (6) 50 cm away from the coring tube.

Cable (3) is connected to the two winglets (7) by means of cable (8).

After implosion the cap-piston system travels up on cable (1) through guide (2),

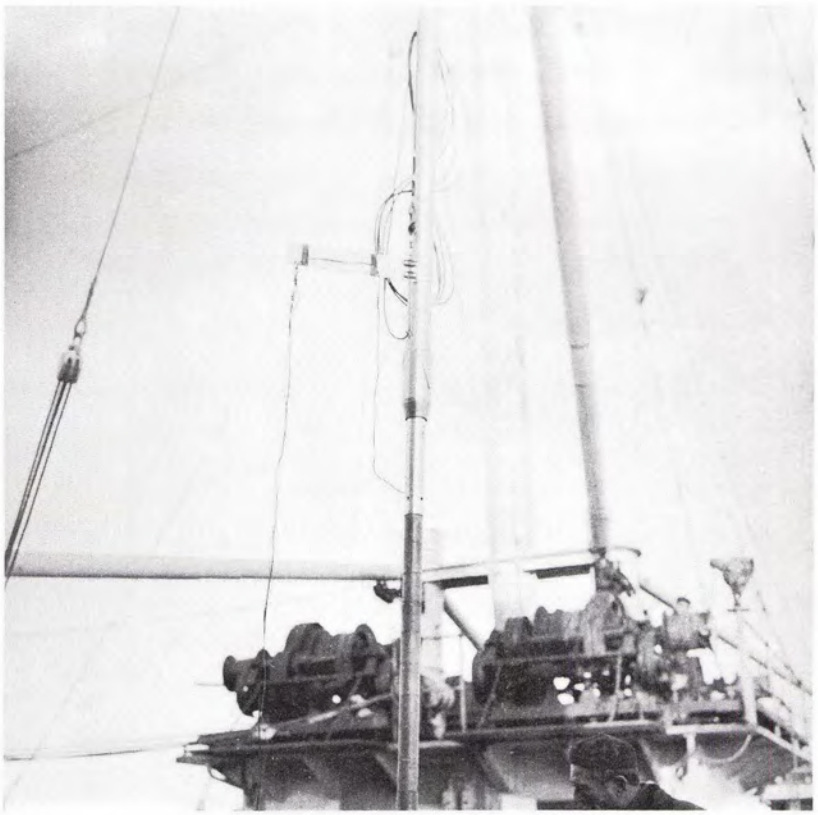

Fig. 18 The Hydrostatic Corer Suspended on Deck of ARAGONESE Before Towing

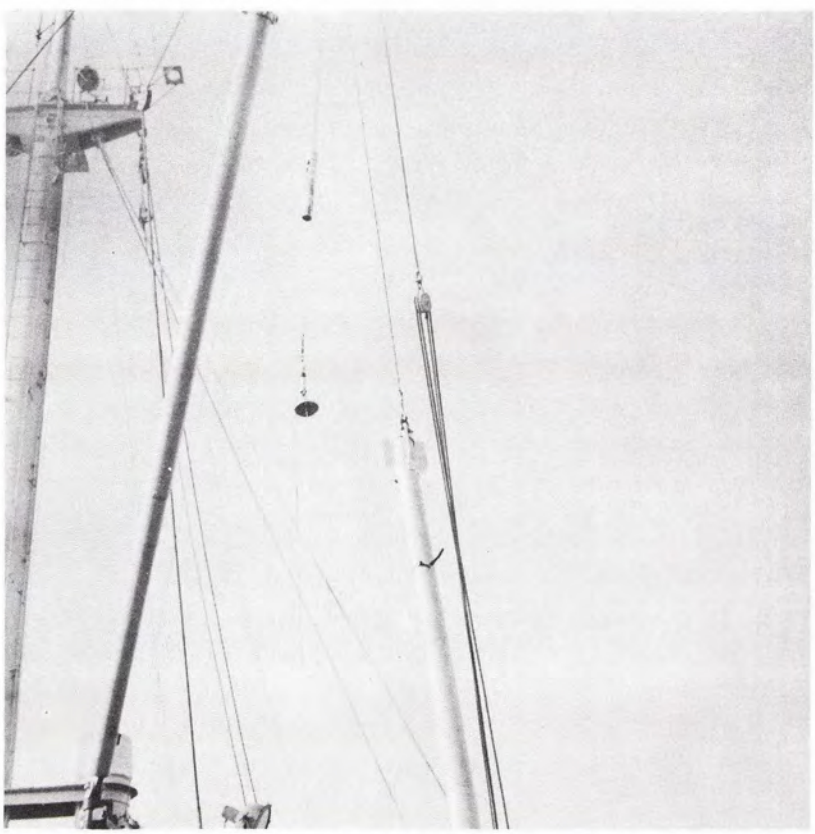

Fig. 19 Recuperation of the Hydrostatic Corer. The Various Parts are Connected to the Cable after Implosion

it then comes down by its own weight and gets caught in A. The battery arm remains connected to the recuperating cable (3).

3. SEA TRIALS

Seven tests were performed between depths of 105 and 215 m; four were successful, and three failed due to small mechanical failures. The first failure was due to the battery case, which sank into the mud and did not tilt the mercury switch. This was prevented later by adding a large base to the lower articulated part of the battery case. The other two failures were due to the piston jamming in the nose, which indicates that too precise fit adjustment between nose and piston should be avoided. The release mechanism seems to have worked correctly all the time.

Of the four successful tests, two were made with the piston weighted with 80 kgs of lead masses. The tube penetrated 3 metres at the first test with this heavy piston. The implosion was easily heard on the Precision Depth Recorder earphones every time a heavy piston was used.

The last test performed with a heavy piston, although successful in itself, resulted in the loss of the tube-nose. Cable (8) caught in the cap-guide shoulder and the 6 mm cable (8) broke at the end of the implosion. The piston, cap, and battery case were recovered normally.

Figure 18 shows the corer mounted on the deck of the oceanographic ship ARAGONESE. The top part of the corer with guiding system is not shown.

Figure 19 shows the various parts of the corer connected to the wire after implosion at 215 m depth. The guided cap and the arm (4) of the battery case wire are not seen on the picture. The piston was not weighted and wire (9) was replaced by a chain. The chain was badly damaged during the implosion, which proves

that little water enters the tube during the propulsion period.

4. TEST CONCLUSIONS

Although more tests at greater depth are needed to prove the real feasibility of the corer, the mechanical arrangement of the prototype seems to be good. As stated before, a catching system will replace cable (9). However, the amount of water entering the tube during the implosion at great marine depth must be accurately known.

The piston should be made of a different material than the one used for the nose.

The technological aspects of the tool must be simplified before it becomes operational.

In the setup of equation of motion for the propulsion phase, Bernouilli's theorem was applied to Eq. (7).

It will be noted that the simplified form of Bernouilli's theorem (see Section 3) is valid only in the case of steady flow and one can then write

$$\frac{p_o}{\rho g} + \frac{v^2}{2g} + h = \frac{p'}{\rho g} + \frac{v'^2}{2g} + h'$$

The equation of motion represents a transient phenomenon and to be correct the generalised Bernouilli's theorem should have been used; that is, if (ds) is a streamline element

$$\frac{p_o}{\rho g} + \frac{1}{g}\int \frac{\partial v}{\partial t}\, ds + \frac{v^2}{2g} + h = \frac{p'}{\rho g} + \frac{1}{g}\int \frac{\partial v'}{\partial t}\, ds + \frac{v'^2}{2g} + h' \qquad (2\text{-}1)$$

Let us call A_1 the horizontal cross section of the total stream of water close to the cap of the tube and A_2 the cross section of the total stream at a distance (s) from the cap on a vertical axis.

If w_1 is the vertical speed of water corresponding to section A_1 and w_2 the vertical speed of water corresponding to section A_2, an equation of continuity can be written

$$A_1 w_1 = A_2 w_2$$

$$w_2 = \frac{A_1}{A_2} w_1$$

The quotient $\frac{A_1}{A_2}$ is a function of (s) and therefore

$w_2 = \phi_{(s)} w_1$, which gives

$$\frac{\partial w_2}{\partial t} = \frac{dw_1}{dt} \phi(s)$$

$$\int \frac{\partial w_2}{\partial t} ds = \frac{dw_1}{dt} \int \phi(s) ds$$

$\int \phi(s) ds$ has the dimension of a length; then we shall write:

$$\int \frac{\partial w_2}{\partial t} ds = \frac{dw_1}{dt} L$$

w_1 is the speed of water in contact with the cap. Transposing this result in equation (17) with $v = 0$ and neglecting the variation of static head, one can write

$$p_o = p' + \frac{v'^2 \rho}{2} + L\rho \frac{dv'}{dt}$$

$$p' = p_o - \frac{v'^2 \rho}{2} - L\rho \frac{dv'}{dt}$$

Equation (3) then becomes

$$m \frac{d^2x}{dt^2} = p_o s - \left(k + \frac{\rho}{2} S\right) \left(\frac{dx}{dt}\right)^2 - L\rho S \frac{dv}{dt}$$

$$(m + L\rho S) \frac{d^2x}{dt^2} = p_o S - \left(k + \frac{\rho}{2} S\right) \left(\frac{dx}{dt}\right)^2$$

The final equation of motion would then be

$$\left(\frac{dx}{dt}\right)^2 = \frac{p_o S}{k + \frac{\rho}{2} S} \left[1 - \exp\left(- \frac{2k + \rho S}{m + L\rho S} x\right)\right]$$

The term $L\rho S$ can be of the order of magnitude of m; for instance, for L = 400 cm (total length of the tube) $L\rho S$ becomes for the full scale prototype: 1 x 400 x 40 = 16000 gm. However, it is expected that L will be much smaller and then ρ LS becomes negligible relatively to m.

In any case as soon as a flow diagram is obtainable, the validity of the hypothesis made in this report will have to be checked.

BIBLIOGRAPHY

1. M. Knudsen, "A Bottom Sampler for Hard Bottom," Medd. fra komm. for havundersögelser - Serie fiskeri Bd. VIII København 1927.

2. H.Pettersson and B.Kullenberg,"A Vacuum Core-Sampler for Deep Sea Sediments," Nature, Vol. 145, 1940, p. 306.

3. C.S. Piggot, "Factors Involved in Submarine Core Sampling," Bull Geol. Soc.Am., Vol. 52, Oct. 1941.

4. K.O. Emery and R.S. Dietz, "Gravity Coring Instrument and Mechanics of Sediment Coring," Bull. Geol. Soc. Am., Vol. 52, Oct. 1941, pp.1685-1714.

5. J. Hvorslev, "Free Fall Coring Tube," Bull. Geol. Soc.Am., Vol. 57, No.10, Oct. 1946.

6. B. Kullenberg, "Deep Sea Coring," Reports of the Sweedish Deep Sea Expedition 1947-1948, Vol. 4, Bottom Investigations, Fasc. 1.

7. H. Pettersson,"Oceanographic Work in the Mediterranean," The Geographical J., Vol. CVII, Nos. 3-4, March-April 1946.

8. C.S. Piggot, "Apparatus to Secure Core Samples from the Ocean-Bottom," Bull. Geol. Soc.Am., Vol. 47, No. 5, May 1936.

9. L. Prandtl and O.G. Tietjens, "Fundamentals of Hydro and Aeromechanics," Dover Public. New York, 1957.

10. W. Taylor, "Fundamentals of Soil Mechanics," John Wiley and Sons Publishers, 1962.

11. K. Terzaghi, and R. Peck, "Soil Mechanics in Engineering Practice," John Wiley and Sons Publishers, 1962.

12. H. Pettersson and B. Kullenberg, "Vakumlodet," Medd. oc. Inst. Göteborg, No. 5, 1941.

DISTRIBUTION LIST

Minister of Defense Brussels, Belgium	10 copies
Minister of National Defense Department of National Defense Ottawa, Canada	10 copies
Chief of Defense, Denmark Kastellet Copenhagen Ø, Denmark	10 copies
Minister of National Defense Division Transmissione-Ecoute-Radar 51 Latour Maubourg Paris 7e, France	10 copies
Minister of Defense Federal Republic of Germany Bonn, Germany	10 copies
Minister of Defense Athens, Greece	10 copies
Ministry of National Defense Navy General Staff Rome, Italy	10 copies
Minister of National Defense Plein 4, The Hague, Netherlands	10 copies
Minister of National Defense Storgaten 33, Oslo, Norway	10 copies
Minister of National Defense, Portugal Care Portuguese Military Attaché 3 Rue Noisiel Paris, France	10 copies
Minister of National Defense Ankara, Turkey	10 copies
Minister of Defense London, England	18 copies
Supreme Allied Commander Atlantic (SACLANT) Norfolk 11, Virginia	5 copies
SACLANT Representative in Europe (SACLANTREPEUR) Place du Marechal de Lattre de Tassigny Paris 16e, France	1 copy
Commander in Chief Western Atlantic Area (CINCWESTLANT) Norfolk 11, Virginia	1 copy
Commander in Chief Eastern Atlantic Area (CINCEASTLANT) Eastbury Park, Northwood Middlesex, England	1 copy
Maritime Air Commander Eastern Atlantic Area (COMAIREASTLANT) R.A.F. Northwood Middlesex, England	1 copy
Commander Submarine Force Eastern Atlantic (COMSUBEASTLANT) Fort Blockhouse Gosport, Hants, England	1 copy
Commander, Canadian Atlantic (COMCANLANT) H.M.C. Dockyard Halifax, Nova Scotia	1 copy
Commander Ocean Sub-Area (COMOCEANLANT) Norfolk 11, Virginia	1 copy
Supreme Allied Commander Europe (SACEUR) Paris, France	7 copies
SHAPE Air Defence Technical Center P.O. Box 174 Stadhouders Plantsoen 15 The Hague, Netherlands	1 copy
Allied Commander in Chief Channel (CINCCHAN) Fort Southwick, Fareham Hampshire, England	1 copy
Commander Allied Maritime Air Force Channel (COMAIRCHAN) Northwood, England	1 copy
Commander in Chief Allied Forces Mediterranean (CINCAFMED) Malta, G.C.	1 copy
Commander South East Mediterranean (COMEDSOUEAST) Malta, G.C.	1 copy

Commander Central Mediterranean
(COMEDCENT)
Naples, Italy — 1 copy

Commander Submarine Mediterranean
(COMSUBMED)
Malta, G.C. — 1 copy

Standing Group, NATO
(SGN)
Room 2C256, The Pentagon
Washington 25, D.C. — 3 copies

Standing Group Representative
(SGREP)
Place du Marechal de Lattre de Tassigny
Paris 16e, France — 5 copies

National Liaison Representatives

NLR Belgium
Belgian Military Mission
3330 Garfield Street, N.W.
Washington, D.C. — 1 copy

NLR Canada
Canadian Joint Staff
2450 Massachusetts Avenue, N.W.
Washington, D.C. — 1 copy

NLR Denmark
Danish Military Mission
3200 Whitehaven Street, N.W.
Washington, D.C. — 1 copy

NLR France
French Military Mission
1759 "R" Street, N.W.
Washington, D.C. — 1 copy

NLR Germany
German Military Mission
3215 Cathedral Avenue, N.W.
Washington, D.C. — 1 copy

NLR Greece
Greek Military Mission
2228 Massachusetts Avenue, N.W
Washington, D.C. — 1 copy

NLR Italy
Italian Military Mission
3221 Garfield Street, N.W.
Washington, D.C. — 1 copy

NLR Netherlands
Netherlands Joint Staff Mission
1470 Euclid Street, N.W.
Washington, D.C. — 1 copy

NLR Norway
Norwegian Military Mission
2720 34th Street, N.W.
Washington, D.C. — 1 copy

NLR Portugal
Portuguese Military Mission
2310 Tracy Place, N.W.
Washington, D.C. — 1 copy

NLR Turkey
Turkish Joint Staff Mission
2125 LeRoy Place, N.W.
Washington, D.C. — 1 copy

NLR United Kingdom
British Defence Staffs, Washington
3100 Massachusetts Avenue, N.W.
Washington, D.C. — 1 copy

NLR United States
SACLANT
Norfolk 11, Virginia — 40 copies

Scientific Committee of National Representatives

Dr. J.E. Keyston
Defense Research Board
Department of National Defense
Ottawa, Canada — 1 copy

G. Meunier
Ingenieur en Chef des Genie Maritime
Services Technique des Constructions et Armes Navales
8 Boulevard Victor
Paris 15e, France — 1 copy

Dr. E. Schulze
Bundesministerium der Verteidigung
ABT H ROMAN 2/3
Bonn, Germany — 1 copy

Commander A. Pettas
Ministry of National Defense
Athens, Greece — 1 copy

Professor Dr. Maurizio Federici
c/o MARICOMITARMI
Ministero della Marina
Rome, Italy — 1 copy

Dr. M.W. Van Batenburg
Physisch Laboratorium RVO-TNO
Waalsdorpvlakte
The Hague, Netherlands — 1 copy

Mr. A.W. Ross
Department of Physical Research
Admiralty, Whitehall
London S.W. 1, England — 1 copy

Dr. J.E. Henderson
Department of Physics
University of Washington
Seattle 5, Washington — 1 copy

CC R. C. Lambert
Etat Major Général Force Navale
Caserne Prince Baudouin
Place Dailly
Bruxelles, Belgique — 1 copy

CAPT H. L. Prause
Sóvaernets Televaesen
Lergravsvej 55
Copenhagen S[1], Denmark — 1 copy

Mr. F. Lied
Norwegian Defense Research
Establishment
Kjeller, Norway — 1 copy

Ing. CAPT N. Berkay
Seyir Ve HDR D
CUBUKLU
Istanbul, Turkey — 1 copy

Dr. P. M. Fye
Woods Hole Oceanographic
Institution
Woods Hole, Mass. — 1 copy

Mr. Sv. F. Larsen
Danish Defense Research Board
Østerbrogades Kaserne
Copenhagen Ø, Denmark — 1 copy

CDR R. J. M. Sabatier
EMM/TER
2 Rue Royale
Paris 8e, France — 1 copy

CF V. Gioncada
Stato Maggiore della Marina
Roma, Italy — 1 copy

CDR F. J. Kelley
Box 39, Navy No. 100
U.S. Navy — 1 copy

ASG for Scientific Affairs
NATO
Porte Dauphine
Paris 16e, France — 1 copy